DFT Investigation of CO Adsorption on Pt(211) and Pt(311) Surfaces from Low to High Coverage

Hideo Orita*,† and Yasuji Inada‡

Research Institute for Computational Sciences (RICS), National Institute of Advanced Industrial Science and Technology (AIST), Tsukuba Central 5, 1-1-1 Higashi, Tsukuba, Ibaraki 305-8565, Japan, and Accelrys K.K., Nishishinbashi TS Building, 3-3-1 Nishishinbashi, Minato-ku, Tokyo 105-0003, Japan

Received: May 17, 2005; In Final Form: September 15, 2005

Adsorption of CO on Pt(211) and Pt(311) surfaces has been investigated by the density functional theory (DFT) method (periodic DMol[3]) with full geometry optimization. Adsorption energies, structures, and C−O stretching vibrational frequencies are studied by considering multiple possible adsorption sites and comparing them with the experimental data. The calculated C−O stretching frequencies agree well with the experimental ones, and precise determination of adsorption sites can be carried out. For Pt(211), CO adsorbs at the atop site on the step edge at low coverage, but CO adsorbs at the atop and bridge sites simultaneously on both the step edge and the terrace with further increasing CO coverage. The present results interpret the reflection adsorption infrared (RAIR) spectra of Brown and co-workers very well from low to high coverage. For Pt(311), CO adsorbs also at the atop site on the step edge at low coverage. The lifting of reconstruction by CO adsorption occurs also for Pt(311), whereas the energy gain for lifting the reconstruction of the Pt(311) surface is smaller than that for Pt(110). The largest difference between the stepped Pt(211)/Pt(311) and Pt(110) surfaces is the occupation on the edge sites at higher coverage. For the stepped surfaces, the bridge site begins to be occupied at higher coverage, whereas the atop site is always occupied for the Pt(110) surface.

1. Introduction

Studying the adsorption of molecules on the surfaces of well-defined stepped and kinked single crystals is an important step toward understanding the role of defects in surface science and catalysis.[1] Various types of steps, kinks, and terraces on single crystals can be obtained by cutting the crystal to a particular orientation. The electronic structure of the steps is usually different from that of the terraces. It is generally accepted that the adsorption energy of molecules on the steps is larger than that on the terraces due to the higher unsaturated coordination at the step sites.[2−4] Therefore, molecules adsorbed on the steps will have different properties from those on the terraces, and it will be possible to distinguish between molecules adsorbed on the steps and the terraces.

The Pt(211) surface is one of the stepped surfaces that are investigated most extensively and is denoted [3(111)×(100)] in step notation (see Figure 1). The (211) surface consists of three-atom-wide terraces with (111) structure and one-atom-high steps with (100) character. The (111) and (100) microfacets decline from the macroscopic (211) surface plane by 19.5 and −35.3°, respectively. There are several extensive studies concerning CO adsorption on Pt(211) experimentally.[5−9] Yates and co-workers have used several different experimental techniques to investigate CO adsorption on Pt(211)[5−8] including reflection adsorption infrared spectroscopy (RAIRS), temperature programmed desorption (TPD), electron stimulated desorption ion angular distribution (ESDIAD), and low energy electron diffraction (LEED). They have found that CO adsorbs at the atop sites on the step edge at low coverage and a small amount of CO begins to adsorb at the bridge sites on the step edge at higher coverage. Atop and bridge sites on the terrace are filled as the CO coverage increases further. However, they could not easily differentiate between CO species adsorbed at the atop sites on the step and the terrace by RAIRS. On the other hand, TPD clearly shows the presence of two desorption peaks at ∼400 and 500 K, which are assigned to the desorption

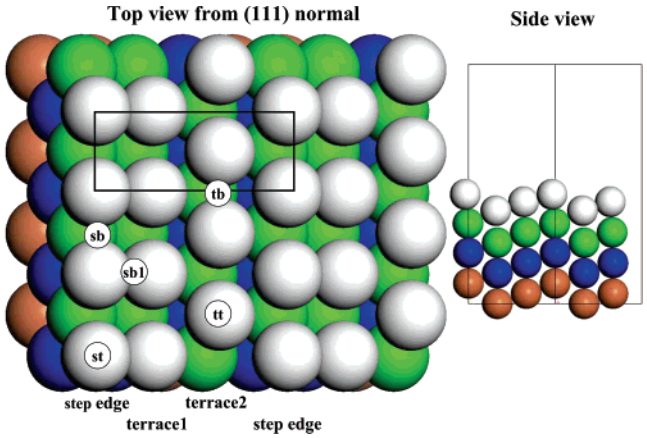

Figure 1. (left) Illustration of adsorption sites on the (211) surface in the top view from the (111) normal with the (1×1) unit lattice. The metal rows on the surface are classified into three types of step edge, terrace1, and terrace2 by coordinate numbers of 7, 10, and 9, respectively. Adsorption sites are abbreviated as the following: st, atop site on step edge; sb, bridge site on step edge; sb1, bridge site perpendicular to step edge; tt, atop site on terrace2; tb, bridge site between two terrace2 atoms. (right) Side view of the (211) surface with the unit cell lattice.

* To whom correspondence should be addressed. Fax: +81-29-861-9291. Phone: +81-29-861-4835. E-mail: hideo-orita@aist.go.jp.
† National Institute of Advanced Industrial Science and Technology (AIST).
‡ Accelrys K.K.

10.1021/jp052583a CCC: $30.25
Published on Web 10/22/2005

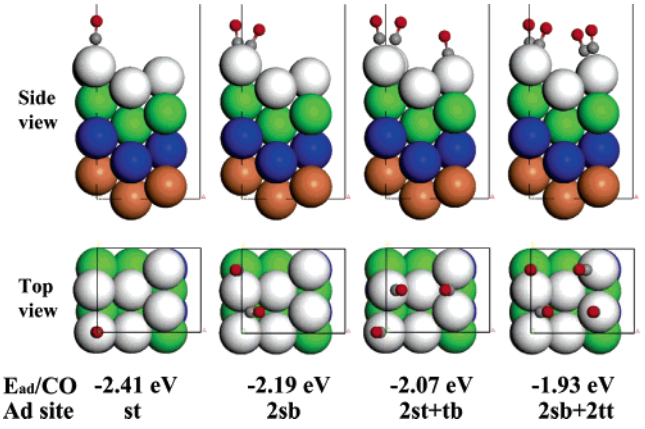

Figure 2. Typical adsorption structures of CO on Pt(211) in the (2×1) unit cell.

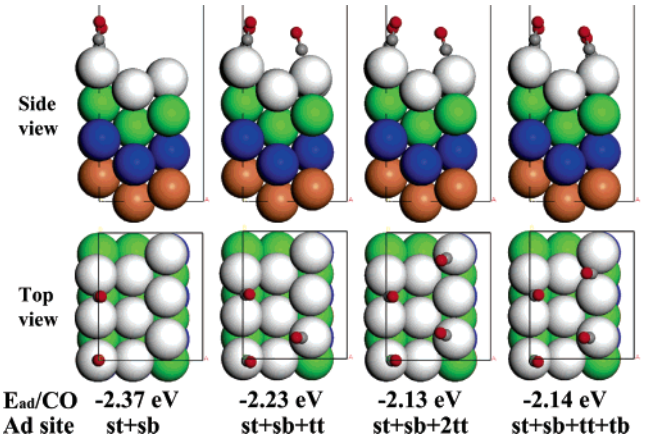

Figure 3. Typical adsorption structures of CO on Pt(211) in the (3×1) unit cell.

of CO from terrace and step sites, respectively. Brown and co-workers have also performed an experiment with RAIRS and TPD by changing the adsorption temperature to reinvestigate CO adsorption on Pt(211) carefully.[9] At 106 K, they have observed four different frequency peaks with RAIRS and assigned them to the atop and bridge CO species adsorbed at step and terrace sites. Adsorption at 330 K produces very similar RAIR spectra, although no peak due to the bridge CO on the terrace is observed. The lack of this peak following adsorption at 330 K is assigned to the larger diffusion rate of CO on the surface at this temperature, which allows the CO to diffuse to more stable sites.

The (311) surface ([2(111)×(100)] in step notation) has two-atom-wide (111) terraces, and each unit cell contains only one terrace atom and one step atom (cf. Figure 5). The (111) and (100) microfacets decline from the macroscopic (311) surface plane by 29.5 and −25.3°, respectively. A clean surface of Pt-(311) exhibits a missing row (1×2) reconstruction, whereas no reconstruction occurs for Pt(211). This reconstruction is lifted to form a (1×1) un-reconstructed surface by CO adsorption.[10] The reconstruction and the lifting process are very similar to those reported for CO on the Pt(110)−(1×2) surface: at low coverage, CO adsorption occurs on the (1×2) surface, but the reconstruction is lifted at higher coverage.[11]

There is still a controversy about predicting the same preference of adsorption sites as inferred from experiments by density functional theory (DFT) (please refer to two recent reviews[12,13] published after a paper of Feibelman et al.[14] which describes that DFT tends to favor adsorption sites with higher coordination). One possible way to check the predicted site

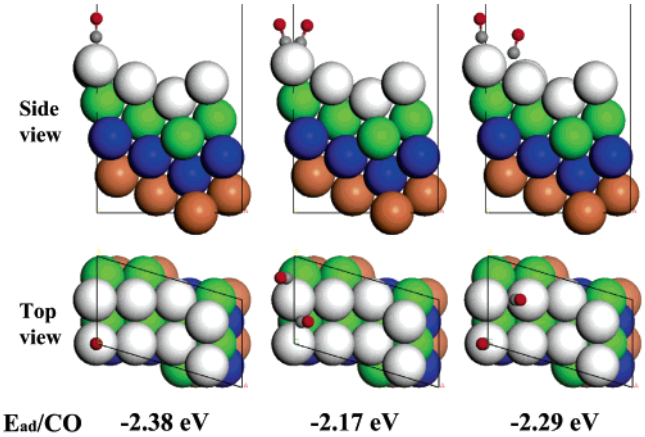

Figure 4. Typical adsorption structures of CO on Pt(311) in the reconstructed (2×2) unit cell.

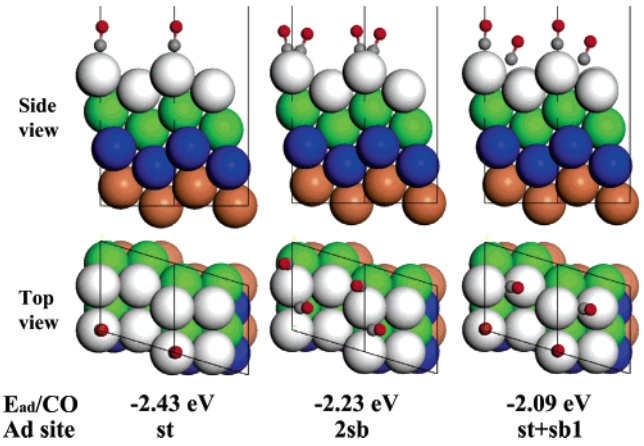

Figure 5. Typical adsorption structures of CO on Pt(311) in the un-reconstructed (2×1) unit cell. Two unit cells are shown to compare them with adsorption structures in the reconstructed (2×2) unit cell.

preference is to compare other more reliably computed observables (e.g., vibrational frequencies) with the measured values.[13] In the present work, we have investigated not only adsorption energies and structures but also vibrational frequencies of CO on Pt(211) from low to high coverage up to $^2/_3$ monolayer (ML) (one ML in the present work defines that on top of each Pt atom in the first physical layer a molecule is positioned). Although DFT studies of CO adsorption on Pt(211) have been undertaken already by several research groups[15−17] including ours,[18] these studies are for a low coverage of $^1/_6$ ML and only few frequency calculations have been done. The present calculation results interpret the RAIR spectra of Brown and co-workers[9] very well from low to high coverage. For Pt(311), we have investigated CO adsorption with two surface models—the reconstructed missing row phase and the un-reconstructed phase—and compared the site preference between Pt(211) and Pt(311).

2. Computational Methods

We performed DFT calculations with the program package DMol^3 in Materials Studio (version 2.2) of Accelrys Inc. on personal computers. In the DMol^3 method,[19−21] the physical wave functions are expanded in terms of numerical basis sets. We used the double-numeric quality basis set with polarization functions (DNP). The size of the DNP basis set is comparable to Gaussian 6-31 G**, but the DNP is more accurate than the Gaussian basis set of the same size.[22] The gradient-corrected

GGA functional, developed by Perdew, Burke, and Ernzerhof (PBE),[23] was employed. A Fermi smearing of 0.002 hartree (1 hartree = 27.2114 eV) and a real-space cutoff of 4 Å were used to improve computational performance. Periodic surface slabs of four physical layers' thickness were used, with a 10 Å vacuum region between the slabs. The adsorbate and the two top layers of metal were allowed to relax in all of the geometry optimization calculations without symmetry restriction (i.e., always using *P*1 symmetry). The tolerances of energy, gradient, and displacement convergence were 2×10^{-5} hartree, 4×10^{-3} hartree/Å, and 5×10^{-3} Å, respectively. The max gradient for most of the optimized structures was less than 2×10^{-3} hartree/Å. Adsorption energies were computed by subtracting the energies of the gas-phase CO molecule and surface from the energy of the adsorption system, as shown in eq 1.

$$E_{ad} = E(\text{CO/surface}) - E(\text{CO}) - E(\text{surface}) \qquad (1)$$

With this definition, a negative E_{ad} value corresponds to stable adsorption on the surface.

The experimentally determined Pt lattice constant of 3.924 Å was used for the production of the surfaces. All electron scalar relativistic (AER)[24] calculations were performed, since AER calculations were necessary to obtain the same site preference as that inferred from experiments in the previous work on CO on Pt(111).[25] For the numerical integration, we used the XFINE quality mesh size of the program, which is a nearly saturated mesh for benchmark calculations. The tolerance of self-consistent field (SCF) convergence was 1×10^{-7}. Under the present computational conditions, the error for the Pt bulk lattice constant was only −0.22%, and the energy difference between the bulk unit cell of the experimental lattice constant and that of the calculated lattice constant was −0.0006 eV.[26] Gil et al.[27] have checked the effect of using the experimental lattice constant, instead of the commonly used optimized value for the bulk. They have concluded that there is no significant effect on the difference in adsorption energy between atop and hollow sites. The C−O bond length for free CO molecule was calculated as 1.14 Å, in good agreement with the experimental value 1.13 Å.[28] The binding energy was calculated as 11.97 eV. The value also agrees well with the reported ones (11.66[29] and 11.71[30] eV) by using the PBE functional.

Harmonic vibrational frequencies were calculated with displacement of not only the CO molecules but also the first layer Pt atoms of surfaces, as described in detail previously.[31] To reduce the computationally expensive cost of frequency calculation, density functional semicore pseudopotentials (DSPPs)[32] were employed instead of AER calculations for the AER-geometry-optimized structures. We checked that the frequency difference between the DSPP and AER calculations was less than 10 cm^{-1}. The harmonic frequency of free CO molecule (d(C−O) = 1.14 Å) was calculated as 2127 cm^{-1}. This value is 2.0% smaller than the experimental harmonic value 2170 cm^{-1} and much closer to the anharmonic one (2143 cm^{-1}).[28]

For Pt(211), a (2×1) surface unit cell (including 24 Pt atoms) was chosen to model the adsorption of CO for coverages of $^1/_6$, $^1/_3$, $^1/_2$, and $^2/_3$ ML. A 5×4×1 *k*-point sampling was used. A (3×1) structure (including 36 Pt atoms) was also chosen to model the adsorption of CO for coverages of $^2/_9$, $^1/_3$, and $^4/_9$ ML. A 3×4×1 *k*-point sampling was used.

For Pt(311), a clean surface is reconstructed with a missing row and the adsorption of CO leads to lifting of the Pt surface to the un-reconstructed phase.[10] Therefore, we adopted two models—the reconstructed missing row phase and the un-reconstructed phase. A reconstructed missing row (2×2) surface unit cell (including 32 Pt atoms) was chosen to model the adsorption of CO on the reconstructed surface with coverages of $^1/_8$ and $^1/_4$ ML. A 5×3×1 *k*-point sampling was used. On the other hand, an un-reconstructed (2×1) surface unit cell (including 16 Pt atoms) was chosen to model the adsorption of CO on the un-reconstructed surface with coverages of $^1/_4$ and $^1/_2$ ML. A 5×5×1 *k*-point sampling was used.

3. Results and Discussion

3.1. Pt(211). Brown and co-workers[9] performed a RAIRS study of CO on Pt(211) by changing the adsorption temperature. One peak is seen to grow into the spectrum at 2071 cm^{-1} for low exposure at 106 K. With increasing exposure, the frequency shifts up to a maximum of 2077 cm^{-1}. At the same time, a higher frequency peak also appears at ∼2087 cm^{-1} and shifts up with further increasing exposure to reach a maximum of 2094 cm^{-1} at saturation. The peak at 2071−2077 cm^{-1} is assigned to an atop CO bonded to the step edge, and the peak at 2087−2094 cm^{-1} is assigned to an atop CO bonded to the terrace. These peaks are thought to increase in frequency as a function of increasing exposure owing to the dipole coupling between CO molecules on the surface. Another peak is also observed in the spectra at ∼1880 cm^{-1} for low exposure and grows into the spectrum with increasing exposure above 0.2 langmuir, although the intensity of the peak is small compared to that seen for the atop CO species. The peak increases in intensity with increasing CO exposure, and a second peak with higher frequency grows into the spectrum. At saturation, two peaks are observed in the spectrum at ∼1918 and 1888 cm^{-1}. The frequencies of these peaks are as would be expected for CO adsorbed in a bridge site. In agreement with the assignments for the atop species, the higher frequency peak is assigned to bridge bonded CO on the terrace and the lower frequency peak is assigned to bridge bonded CO on the step edge.

We have previously calculated the adsorption energies and structures of CO on Pt(211) in a (2×1) unit cell only at $^1/_6$ ML of CO coverage.[18] In the present work, we have extended the previous work by calculating not only adsorption energies and structures but also C−O stretching frequencies for CO in two different unit cells of (2×1) and (3×1) from low to high coverage up to $^2/_3$ ML to assign the RAIR spectra of Brown and co-workers[9] more precisely. Atop and bridge sites as shown in Figure 1 are investigated because 3-fold hollow sites (hexagonal close-packed (hcp) and face-centered cubic (fcc)) are less stable than the atop and bridge sites according to our previous study.[18] The calculated adsorption energies, structures, and stretching frequencies are listed in Table 1, and typical optimized adsorption structures are shown in Figures 2 and 3. The most favorable adsorption occurs at the st site with an E_{ad} value of −2.41 eV/CO (for the abbreviations of the adsorption sites, see the caption of Figure 1). The C−O stretching frequency is calculated as 2052 cm^{-1}. This result agrees with that of the experiment performed by Brown and co-workers[9] because their observed C−O stretching frequency for low exposure up to 0.2 langmuir (2071−2073 cm^{-1}) shows that CO adsorbs at the atop site on the step edge of the surface. The C−O stretching frequency for the second favorable adsorption site of sb is calculated as 1864 cm^{-1}. Because there is no peak lower than 1950 cm^{-1} until the exposure reaches 0.2 langmuir, the sb site is not populated for low exposure, whereas the energy difference between the st and sb sites is 0.09 eV/CO. The C−O stretching frequency for tt is calculated as 2087 cm^{-1}, and it is worth noting that this frequency is a little higher than that for st.

Karmazyn et al.[15] have mentioned that Kose measured the adsorption heat of CO on Pt(211) calorimetrically in his Ph.D.

TABLE 1: Adsorption Energies, Structures, and Stretching Frequencies for CO on the Pt(211) Surface

ad site	E_{ad}[a]/eV	d(Pt−C)/Å	d(C−O)/Å	tilt angle[b]/deg	ν(CO)/cm^{-1}
		(2×1) Structure			
$^1/_6$ ML					
st	**−2.41**	**1.83**	**1.16**	**−2.7**	**2052**
sb	−2.32	2.01, 2.01	1.18	−11.3	1864
tt	−1.97	1.83	1.16	17.1	2087
tb	−1.85	2.02, 2.03	1.18	15.4	1867
sb1	−1.97	1.98, 2.03	1.18	−28.9	1871
$^1/_3$ ML					
2st	−2.14	1.84, 1.84	1.16, 1.16	−22.5, 12.3	2071, 2007
2sb	**−2.19**	**2.02, 2.02, 2.02, 2.02**	**1.18, 1.18**	**−28.0, 7.6**	**1929, 1856**
st+tt	−2.17	st:1.83	1.16	−12.0	2089, 2026
		tt: 1.83	1.16	17.0	
st+tb	−2.10	st:1.83	1.16	−5.8	2067, 1828
		tb: 2.03, 2.04	1.18	16.5	
st+sb1	−2.11	st: 1.84	1.16	2.4	2073, 1852
		sb1: 1.96, 2.04	1.18	−28.6	
sb+tt	−2.14	sb: 2.01, 2.01	1.19	−11.5	2093, 1843
		tt: 1.84	1.15	18.6	
$^1/_2$ ML					
2sb+tt-I	−2.07	sb: 2.01, 2.01	1.18	−20.9	2068, 1897,
		2.02, 2.02	1.18	8.5	1831
		tt: 1.84	1.15	10.6	
2sb+tt-II	−2.07	sb: 2.01, 2.01	1.18	−26.9	2082, 1912,
		2.02, 2.02	1.18	3.9	1847
		tt: 1.84	1.15	20.5	
2st+tb	−2.07	st: 1.84, 1.84	1.16, 1.16	−17.4, 11.6	2085, 2022,
		tb: 2.01, 2.01	1.18	11.5	1846
2st+tt	−2.06	st: 1.83, 1.84	1.16, 1.16	−19.8, 5.3	2101, 2044,
		tt: 1.82	1.16	15.8	2002
$^2/_3$ ML					
2sb+2tt	**−1.93**	**sb: 2.01, 2.01, 2.02, 2.02**	**1.18, 1.18**	**−22.9, 3.9**	**2106, 2051**
		tt: 1.84, 1.84	**1.15, 1.15**	**4.8, 24.2**	**1891, 1830**
2st+2tb	−1.88	st: 1.84, 1.84	1.16, 1.15,	−22.4, 4.0	2100, 2040
		tb: 2.02, 2.02, 2.02, 2.02	1.18, 1.18	5.2, 24.7	1865, 1815
2st+2tt	−1.90	st: 1.84, 1.83	1.16, 1.16	−16.8, 2.7	2113, 2046
		tt: 1.83, 1.83	1.16, 1.16	15.7, 15.9	2032, 2003
		(3×1) Structure			
$^2/_9$ ML					
2st	−2.34	1.83, 1.84	1.16, 1.16	−14.4, 7.4	2058, 2019
2sb	−2.26	1.97, 2.08	1.18	−12.1	1889, 1844
		1.98, 2.07	1.18	−3.2	
st+tt	−2.19	st: 1.83	1.16	−4.9	2085, 2043
		tt: 1.83	1.16	16.7	
st+sb1	−2.14	st: 1.84	1.16	−5.4	2041, 1847
		sb1: 1.98, 2.04	1.18	−28.1	
st+sb	**−2.37**	**st: 1.84**	**1.16**	**−2.4**	**2066, 1833**
		sb: 2.01, 2.01	**1.18**	**−6.4**	
$^1/_3$ ML					
st+sb+tt	**−2.23**	**st: 1.84**	**1.16**	**−11.1**	**2091, 2043,**
		sb: 2.01, 2.01	**1.18**	**−11.9**	**1851**
		tt: 1.83	**1.15**	**17.6**	
2st+tb	−2.17	st: 1.84, 1.84	1.16, 1.16	−9.5, −8.7	2065, 2030,
		tb: 2.02, 2.02	1.18	15.0	1832
2sb+tt	−2.18	sb: 1.98, 2.08	1.18	−12.0	2097, 1883,
		1.98, 2.07	1.18	−12.3	1843
		tt: 1.83	1.15	17.5	
st+sb+tb	−2.18	st: 1.84	1.15	−6.6	2074, 1871,
		sb: 2.00, 2.02	1.18	−12.2	1835
		tb: 2.02, 2.03	1.18	16.1	
3st	−2.15	st: 1.83	1.16	−3.6	2081, 2025,
		1.83	1.16	−24.9	2022
		1.84	1.16	17.0	
3sb	−2.15	sb: 2.02, 2.02	1.18	−22.5	1918, 1862,
		2.01, 2.03	1.18	3.9	1852
		2.01, 2.03	1.18	4.8	
$^4/_9$ ML					
st+sb+2tt	−2.13	st: 1.84	1.16	−11.7	2083, 2049,
		sb: 2.01, 2.01	1.18	−10.9	2022, 1845
		tt: 1.83, 1.83	1.16, 1.16	18.4, 18.7	
st+sb+tt+tb	−2.14	st: 1.84	1.16	−10.4	2098, 2052,
		sb: 2.00, 2.02	1.18	−12.3	1864, 1830
		tt: 1.83	1.15	17.1	
		tb: 2.02, 2.02	1.18	15.8	
free CO			1.14		2139

[a] Adsorption energy per CO molecule. [b] Tilt angle stands for the angle of the C−O axis from the macroscopic (211) normal. Negative and positive tilt angles show that the CO molecule tilts downward to the (100) normal and upward to the (111) normal, respectively.

thesis. He found that it decreases from an initial value of 1.92 eV to 1.58 eV at a coverage of 0.17 ML (it should be noted that in the papers of King and co-workers they are using "apparent coverage" but not absolute coverage and that their apparent coverage for the (211) surface equals 3 times that of the absolute coverage used in the present work) and then finally to a minimum value of ~1 eV at a coverage of 0.5 ML. The initial adsorption heat for Pt(211) is quite similar to that for Pt(111) (−1.90 eV),[33] although TPD spectra clearly show that CO adsorbs more strongly on Pt(211) than Pt(111).[5,8,9,17] For Pt(211), two desorption peaks exist clearly at ~400 and 500 K, and these peaks are assigned to the desorption of CO from terrace and step sites, respectively. The difference of peak temperature of 100 K in the TPD spectrum leads to the difference of desorption energy of ~0.3 eV when the desorption energy is estimated by using Redhead's method[34] with a preexponential factor of 10^{13} s^{-1}. Although the absolute values of the calculated adsorption energies are overestimated, the relative energy difference between the terrace and step sites is closer in comparison with the experimental ones (i.e., 0.4 eV (calculation) vs 0.3 eV (experiment)). When using the rPBE functional,[35] the adsorption energies of the st and sb species at $^1/_6$ ML decrease to −2.13 and −1.99 eV/CO, respectively. The relative energy difference between the two sites remains almost unchanged (i.e., 0.09 eV (PBE) vs 0.14 eV (rPBE)). Therefore, the relative energy difference among the sites is the most important parameter for comparing the properties of adsorption sites.

The most favorable adsorption for $^1/_3$ ML in the (2×1) unit cell occurs for the 2sb configuration with an E_{ad} value of −2.19 eV/CO and C−O stretching frequencies of 1929 and 1856 cm^{-1}, whereas the RAIR spectra of Brown and co-workers[9] show the frequency peaks higher than 2050 cm^{-1} dominate the spectrum. The energy difference from the second favorable configuration of st+tt is only 0.02 eV/CO. The difference of adsorption energy between $^1/_3$ and $^1/_6$ ML is a little large (0.22 eV/CO). Furthermore, Henderson et al. have reported that a (3×1) LEED pattern is observed at 0.53 ML[5] (their saturation coverage of 0.79 ML might be a little overestimated, as discussed later), so we should examine adsorption configurations at coverages around $^1/_3$ ML more carefully by using a larger (3×1) unit cell.

For $^2/_9$ ML in the (3×1) unit cell, the most favorable adsorption occurs for the st+sb configuration with an E_{ad} value of −2.37 eV/CO. The second favorable adsorption occurs for the 2st configuration with an E_{ad} value of −2.34 eV/CO, and the energy difference from the st+sb configuration is only 0.03 eV/CO. The C−O stretching frequencies of the st+sb and 2st configurations are calculated as 2066/1833 cm^{-1} (st+sb) and 2058/2019 cm^{-1} (2st), respectively. The higher frequency mode is symmetric, dipole active, and visible in IR measurements: two CO molecules vibrate in the same direction. The lower one is asymmetric and dipole less active mode: two CO molecules vibrate in opposite directions.

For $^1/_3$ ML in the (3×1) unit cell, CO molecules adsorb most favorably for the st+sb+tt configuration with an E_{ad} value of −2.23 eV/CO, and this adsorption energy is a little larger than that of the most stable configuration for $^1/_3$ ML in the (2×1) unit cell (−2.19 eV/CO). The energy difference from the second favorable adsorption of the 2sb+tt or st+sb+tb configurations is 0.05 eV/CO. The C−O stretching frequencies for the st+sb+tt configuration are calculated as 2091 (with the symmetric mode and dipole active mode being visible in the IR measurements: three CO molecules vibrate in the same direction, but the two atop species vibrate more largely than the sb species), 2043 (asymmetric: the two atop species mainly vibrate in opposite directions), and 1851 cm^{-1} (asymmetric: the sb species mainly vibrate). For $^4/_9$ ML in the (3×1) unit cell, two investigated configurations (st+sb+2tt and st+sb+tt+tb) show quite similar adsorption energies (−2.13 and −2.14 eV/CO, respectively). The symmetric and dipole active C−O stretching frequencies are 2083 and 2098 cm^{-1} for these configurations (all four CO molecules in the unit cell vibrate in the same direction, but the atop species mainly vibrate).

These results for the (3×1) unit cell coincide with the explanation of the RAIRS results because CO molecules clearly adsorb at the bridge site on the step edge with increasing exposure, and then CO molecules begin to adsorb at the atop site on the terrace beside the step edge.

Returning to the results in the (2×1) unit cell, all of the configurations investigated for $^1/_2$ ML show similar adsorption energies (I and II in Table 1 indicate the configurations where the tt species is located closer and farther from the sb species tilting downward to the (100) normal, respectively). Therefore, CO molecules adsorb at the atop and bridge sites simultaneously on both the step edge and the terrace at this CO coverage. These results also coincide with the explanation of the RAIRS results because CO molecules begin to adsorb at the bridge site on the terrace finally with further increasing CO exposure.

For $^2/_3$ ML in the (2×1) unit cell, the most favorable adsorption occurs for the 2sb+2tt configuration with an E_{ad} value of −1.93 eV/CO. The C−O stretching frequencies are 2106 (with the symmetric mode and dipole active mode being visible in the IR measurements: four CO molecules vibrate in the same direction, but the two tt species vibrate more largely than the sb species), 2051 (asymmetric: the two atop species mainly vibrate in opposite directions), 1891 (asymmetric: the two sb species mainly vibrate in the same direction), and 1830 cm^{-1} (asymmetric: the two sb species mainly vibrate in opposite directions). As the total energy difference per (2×1) unit cell between this configuration and the second most favorable 2st+2tt configuration becomes 0.12 eV, the sb species instead of the st species mainly occupies the step edge. Furthermore, the highest frequency peak at 2094 cm^{-1} observed by Brown and co-workers[9] should be due to the tt species instead of the st species. The abrupt increase of this highest frequency peak for exposures larger than 2 langmuir can be explained by the change of site occupation from st to sb at high coverage. As shown in Figure 2, the surface is already crowded by CO molecules at $^2/_3$ ML. To achieve a saturation coverage of $^5/_6$ ML estimated by Yates and co-workers,[5] the next CO molecule has to adsorb at one of the sites around the terrace1, whereas these sites have been found to be much less stable even at $^1/_6$ ML.[18] It might be more reasonable to estimate the saturation coverage as $^2/_3$ ML.

The Pt−C and C−O distances for the atop and bridge sites are calculated as 1.82−1.84 Å (atop)/1.96−2.08 Å (bridge) and 1.15−1.16 Å (atop)/1.18−1.19 Å (bridge), respectively. They are quite similar to those calculated previously for Pt(111),[25] while two Pt−C distances for some of the sb species in the (3×1) unit cell become nonequivalent (e.g., the Pt−C distances for the 2sb configuration are 1.97/2.08 and 1.98/2.07 Å). These distances are also in good agreement with the experimental ones for CO on Pt(111) by LEED[36] (Pt−C distance: 1.85 ± 0.1 and 2.08 ± 0.07 Å for the atop and bridge sites, respectively; C−O distance: 1.15 ± 0.05 Å for both of the sites), although there is no report on determination of C−O and Pt−C distances for CO on Pt(211).

TABLE 2: Adsorption Energies and Structures for CO on the Pt(311) Surface in Reconstructed (2×2) and Un-reconstructed (2×1) Unit Cells

ad site	E_{ad}[a]/eV	d(Pt−C)/Å	d(C−O)/Å	tilt angle[b]/deg
Reconstructed Missing Row (2 × 2)				
1/8 ML				
st	**−2.38**	**1.83**	**1.16**	**−1.2**
sb	−2.31	2.01, 2.01	1.18	−4.4
sb1	−2.29	1.98, 2.04	1.18	−16.8
1/4 ML				
2sb	−2.17	2.02, 2.02, 2.02, 2.02	1.18, 1.18	−20.7, 18.6
2st	−2.14	1.84, 1.83	1.16, 1.16	−18.3, 19.7
st+sb1	**−2.29**	**st: 1.84**	**1.16**	**5.4**
		sb1: 1.95, 2.04	**1.18**	**−13.9**
Un-reconstructed (2 × 1)				
1/4 ML				
st	**−2.43**	**1.83**	**1.16**	**−5.5**
sb	−2.39	2.01, 2.02	1.18	−6.2
sb1	−1.96	1.95, 2.07	1.18	−21.2
1/2 ML				
2sb	**−2.23**	**2.01, 2.01, 2.02, 2.02**	**1.18, 1.18**	**−21.9, 10.9**
2st	−2.20	1.83, 1.83	1.16, 1.16	−14.4, 18.6
st+sb1	−2.09	st: 1.84	1.16	−3.5
		sb1: 1.95, 2.04	1.18	−20.3

[a] Adsorption energy per CO molecule. [b] Tilt angle stands for the angle of the C−O axis from the macroscopic (311) normal. Negative and positive tilt angles show that the CO molecule tilts downward to the (100) normal and upward to the (111) normal, respectively.

3.2. Pt(311). A clean surface of Pt(311) exhibits a missing row (1×2) reconstruction, and this reconstruction is lifted to form a (1×1) un-reconstructed surface by CO adsorption above a critical apparent coverage of 0.16 ML.[10] The reconstruction and the lifting process are very similar to those reported for CO on Pt(110)−(1×2): at low coverage, CO adsorption occurs on the (1×2) surface, but above 0.2 ML, the reconstruction is lifted continuously with increasing CO coverage.[11]

We have performed DFT calculations of CO on Pt(311) in reconstructed (2×2) and un-reconstructed (2×1) unit cells at several CO coverages. For 1/4 ML in the un-reconstructed (2×1) unit cell, the results have been reported already.[18] As the three sites (st, sb, and sb1) are stable in the un-reconstructed (2×1) unit cell, only these sites are investigated in the present work. The calculated adsorption energies and structures are listed in Table 2, and typical optimized adsorption structures are shown in Figures 4 and 5.

For 1/8 ML in the reconstructed missing row (2×2) unit cell, the most favorable adsorption occurs at the st site with an E_{ad} value of −2.38 eV/CO. The energy difference from the second most favorable adsorption site of the sb site is 0.07 eV/CO. The sb1 site in the (2×2) unit cell is relatively more stable than that in the un-reconstructed (2×1) unit cell owing to the larger area of the (100) microfacet. The most stable adsorption for 1/4 ML in the (2×2) structure occurs for the st+sb1 configuration with an E_{ad} value of −2.23 eV/CO. The energy difference from the second most stable adsorption configuration of 2sb is 0.06 eV/CO.

For 1/4 ML in the un-reconstructed (2×1) unit cell, the CO molecule adsorbs most favorably at the st site with an E_{ad} value of −2.43 eV/CO. The second most favorable adsorption site is the sb site with an E_{ad} value of −2.39 eV/CO. On the other hand, the most favorable adsorption for 1/2 ML in the (2×1) unit cell occurs for the 2sb configuration with an E_{ad} value of −2.23 eV/CO. Although the energy difference from the second most favorable adsorption configuration of 2st is only 0.03 eV/CO, the step edge should be occupied mainly by the sb species. At high coverage, the change of site occupation on the step edge occurs from st to sb as mentioned above for Pt(211).

To compare the adsorption energies of CO on Pt(311) for 1/4 ML in the (2×1) and (2×2) unit cells in Table 2, the adsorption energy of the most favorable site for 1/4 ML in the un-reconstructed (2×1) unit cell is 0.14 eV/CO larger than that of the st+sb1 configuration in the reconstructed (2×2) unit cell. On the other hand, we have found that without CO adsorption the reconstructed (2×2) unit cell is more stable than the un-reconstructed (2×1) unit cell by 0.12 eV/(2×1) unit cell. The total energy gain for lifting of the Pt(311) surface to the un-reconstructed phase by CO adsorption is only 0.02 eV/(2×1) unit cell. It is difficult to say whether the lifting of reconstruction occurs or not only by this small energy gain, so the calculation has been re-performed with expansion of the un-reconstructed (2×1) unit cell to the (2×2) unit cell. The energy gain for lifting of reconstruction increases to 0.04 eV/(2×1) unit cell because more relaxation is possible in the larger (2×2) unit cell. Although this value is still smaller than that for Pt(110) (0.19 eV/(2×1) unit cell),[37] the lifting of reconstruction probably occurs also for Pt(311), as reported experimentally by Kose and King.[10]

The adsorption heat of CO on Pt(311) has been measured calorimetrically.[10] The initial heat of adsorption at 300 K is 2.18 eV but drops quickly at an apparent coverage of ∼0.16 ML to reach a plateau for the coverage range from 0.16 to 0.5 ML, where the heat of adsorption is around 2.07 eV. The heat does not significantly change over this range. For coverages very close to 0.5 ML, the heat of adsorption suddenly drops to reach a second plateau. Over the range between 0.5 and 1 ML, the heat of adsorption again remains almost constant with a value of 1.97 eV. At the end of this second plateau, the heat of adsorption undergoes another sudden change to drop off to its steady state value of 1.14 eV, making the beginning of the third plateau (for an apparent coverage above 1 ML). As can be seen in Figure 5, it is reasonable to estimate the saturation coverage for Pt(311) as 1/2 ML. Then, the apparent coverage of Kose and King[10] becomes equal to twice that of the absolute coverage in the present work, so the coverage is shown only with the absolute coverage for convenience later. The first drop of adsorption heat at 0.08 ML should be due to the lifting of the reconstruction. From the LEED experiments of Kose and King,[10] the lifting of the reconstruction occurs over a coverage of 0.1−0.25 ML, which is quite consistent with the present result that the adsorption structure at 1/4 ML is more stable for the un-reconstructed (1×1) phase than the (1×2) reconstructed phase. The second drop of adsorption heat at 0.25 ML should also correspond to the present result that the change of site occupation on the step edge occurs at coverages larger than 1/4 ML. Although our calculated adsorption energies are overestimated in comparison with the experimental results because of the tendency of overestimation in the DFT methods, they agree with each other qualitatively.

The Pt−C and C−O distances for the st and sb sites are calculated as 1.83−1.84 Å (st)/2.01−2.02 Å (sb) and 1.16 Å (st)/1.18 Å (sb), respectively. They are again quite similar to those calculated previously for Pt(111).[25] These distances are also in good agreement with the experimental ones for CO on Pt(111) by LEED,[36] although there is no report on determination of C−O and Pt−C distances for CO on Pt(311).

3.3. Comparison with the Previous Results for Pt(110). A clean surface of Pt(110) is also reconstructed to a (1×2) phase with a missing row, and the adsorption of CO leads to lifting of this reconstruction to a (1×1) phase. According to our previous DFT study,[37] CO adsorbs preferentially at the atop site on the edge for both the reconstructed missing row (1×2) surface and the un-reconstructed (1×1) surface at all coverages up to 1/2 ML. When adjacent sites along the edge row begin to

be occupied, the CO molecules tilt alternately by ~20° from the surface normal in opposite directions for both the (1×2) and (1×1) surfaces. Lifting of reconstruction by CO adsorption is recognized more easily because the energy gain for lifting is larger than that for Pt(311) (0.19 vs 0.04 eV/(2×1) unit cell). The largest difference between the present results for stepped surfaces and the previous ones for Pt(110) is the occupation on the edge sites at higher coverage. For the stepped surfaces, the bridge site begins to be occupied at higher coverage, whereas the atop site is always occupied for Pt(110). Furthermore, the CO molecules on the step edge tend to tilt downward more largely (e.g., the tilt angles of the sb species on Pt(311) for $^1/_2$ ML in the un-reconstructed (2×1) unit cell are −21.9 and 10.9°).

4. Conclusion

Adsorption of CO on Pt(211) and Pt(311) surfaces has been investigated by the density functional theory (DFT) method (periodic DMol[3]) at the generalized gradient approximation (GGA) level with full geometry optimization and without symmetry restriction. Adsorption energies, structures, and C−O stretching vibrational frequencies for these surfaces are studied by considering multiple possible adsorption sites and comparing them with the experimental data. The calculated C−O stretching frequencies agree well with the experimental ones, and precise determination of adsorption sites can be carried out. For Pt(211), CO adsorbs at the atop site on the step edge at low coverage, but CO adsorbs at the atop and the bridge sites simultaneously on both the step edge and the terrace with further increasing CO coverage. The present results interpret the RAIR spectra of Brown and co-workers[9] very well from low to high coverage. For Pt(311), CO adsorbs also at the atop site on the step edge at low coverage. The most stable adsorption for $^1/_4$ ML in the reconstructed (2×2) unit cell occurs for the st+sb1 configuration because the sb1 site becomes more stable owing to the larger area of the (100) microfacet in the reconstructed phase. The lifting of reconstruction by CO adsorption occurs also for Pt(311), whereas the energy gain for lifting of the Pt(311) surface is smaller than that for Pt(110). The largest difference between the stepped Pt(211)/Pt(311) and Pt(110) surfaces is the occupation on the edge sites at higher coverage. For the stepped surfaces, the bridge site begins to be occupied at higher coverage, whereas the atop site is always occupied for Pt(110).

References and Notes

(1) Somorjai, G. A. *Introduction to Surface Chemistry and Catalysis*; Wiley: New York, 1994.

(2) Zubkov, T.; Morgan, G. A., Jr.; Yates, J. T., Jr.; Kühlert, O.; Lisowski, M.; Schillinger, R.; Fick, D.; Jänsch, H. J. *Surf. Sci.* **2003**, *526*, 57 and references therein.

(3) Ge, Q.; Neurock, M. *J. Am. Chem. Soc.* **2004**, *126*, 1551.

(4) Backus, E. H. G.; Eichler, A.; Grecea, M. L.; Kleyn, A. W.; Bonn, M. *J. Chem. Phys.* **2004**, *121*, 7946.

(5) Henderson, M. A.; Szabó, A.; Yates, J. T., Jr. *J. Chem. Phys.* **1989**, *91*, 7245.

(6) Henderson, M. A.; Szabó, A.; Yates, J. T., Jr. *J. Chem. Phys.* **1989**, *91*, 7255.

(7) Szabó, A.; Henderson, M. A.; Yates, J. T., Jr. *J. Chem. Phys.* **1990**, *92*, 2208.

(8) Xu, J.; Yates, J. T., Jr. *Surf. Sci.* **1995**, *327*, 193.

(9) Mukerji, R. J.; Bolina, A. S.; Brown, W. A. *Surf. Sci.* **2003**, *527*, 198.

(10) Kose, R.; King, D. A. *Chem. Phys. Lett.* **1999**, *313*, 1.

(11) Wartnaby, C. E.; Stuck, A.; Yeo, Y. Y.; King, D. A. *J. Phys. Chem.* **1996**, *100*, 12483.

(12) Gajdoš, M.; Eichler, A.; Hafner, J. *J. Phys.: Condens. Matter* **2004**, *16*, 1144.

(13) Neyman, K. M.; Illas, F. *Catal. Today* **2005**, *105*, 2.

(14) Feibelman, P. J.; Hammer, B.; Nørskov, J. K.; Wagner, F.; Scheffler, M.; Stumpf, R.; Watwe, R.; Dumesic, J. *J. Phys. Chem. B* **2001**, *105*, 4018.

(15) Karmazyn, A. D.; Fiorin, V.; Jenkins, S. J.; King, D. A. *Surf. Sci.* **2003**, 538, 171.

(16) Hammer, B.; Nielsen, O. H.; Nørskov, J. K. *Catal. Lett.* **1997**, *46*, 31.

(17) Creighan, S. C.; Mukerji, R. J.; Bolina, B. A.; Lewis, D. W.; Brown, W. A. *Catal. Lett.* **2003**, *88*, 39.

(18) Orita, H.; Itoh, N.; Inada, Y. *Surf. Sci.* **2004**, *571*, 161.

(19) Delley, B. *J. Chem. Phys.* **1990**, *92*, 508.

(20) Delley, B. *J. Phys. Chem.* **1996**, *100*, 6107.

(21) Delley, B. *J. Chem. Phys.* **2000**, *113*, 7756.

(22) Benedek, N. A.; Snook, I. K.; Latham, K.; Yarovsky, I. *J. Chem. Phys.* **2005**, *122*, 144102; *DMol[3] User Guide*; Accelrys Inc.: San Diego, CA, 2003.

(23) Perdew, J. P.; Burke, K.; Ernzerhof, M. *Phys. Rev. Lett.* **1996**, *77*, 3865.

(24) Delley, B. *Int. J. Quantum Chem.* **1998**, *69*, 423.

(25) Orita, H.; Itoh, N.; Inada, Y. *Chem. Phys. Lett.* **2004**, *384*, 271.

(26) When the DNP basis set was expanded to a larger one (e.g., triple numeric quality type one), the calculated bulk lattice constant was always smaller than the experimental one, more than −3% in some cases. Furthermore, calculations for larger surface unit cells such as the (3×1) structure of Pt(211) with the expanded basis sets became much more computationally expensive and sometimes almost impossible.

(27) Gil, A.; Clotet, A.; Ricart, J. M.; Kresse, G.; García-Hernández, M.; Rösch, N.; Sautet, P. *Surf. Sci.* **2003**, *530*, 71.

(28) *CRC Handbook of Chemistry and Physics*, 81st ed.; Lide, D. R., Ed.; CRC Press: Boca Raton, FL, 2000.

(29) Kurth, S.; Perdew, J. P.; Blaha, P. *Int. J. Quantum Chem.* **1999**, *75*, 889.

(30) Ernzerhof, M.; Scuseria, G. E. *J. Chem. Phys.* **1999**, *110*, 5029.

(31) Orita, H.; Nakamura, I.; Fujitani, T. *Surf. Sci.* **2004**, *571*, 102.

(32) Delley, B. *Phys. Rev. B* **2002**, *66*, 155125.

(33) Yeo, Y. Y.; Vattuone, L.; King, D. A. *J. Chem. Phys.* **1997**, *106*, 392.

(34) Redhead, R. A. *Trans. Faraday Soc.* **1961**, 57, 641; *Vacuum* **1962**, *12*, 203.

(35) Hammer, B.; Hansen, L. B.; Nørskov, J. K. *Phys. Rev. B* **1999**, *59*, 7413.

(36) Ogletree, D. F.; van Hove, M. A.; Somorjai, G. A. *Surf. Sci.* **1986**, *173*, 351.

(37) Yamagishi, S.; Fujimoto, T.; Inada, Y.; Orita, H. *J. Phys. Chem. B* **2005**, *109*, 8899.